Chemical Geology 459 (2017) 24–31

Contents lists available at ScienceDirect

Chemical Geology

journal homepage: www.elsevier.com/locate/chemgeo

In-situ determination of the kinetics and mechanisms of nickel adsorption by nanocrystalline vernadite

Sylvain Grangeon[a,*], Alejandro Fernandez-Martinez[b,c], Francis Claret[a], Nicolas Marty[a], Christophe Tournassat[a], Fabienne Warmont[d], Alexandre Gloter[e]

[a] BRGM, 3 avenue Claude Guillemin, 45060 Orléans Cedex 2, France
[b] University Grenoble Alpes, ISTerre, 38041 Grenoble, France
[c] CNRS, ISTerre, 38041 Grenoble, France
[d] ICMN-CNRS-Université d'Orléans, 1b rue de la Férollerie, 45071 Orléans Cedex 2, France
[e] Laboratoire de Physique des Solides, Université Paris-Sud, CNRS UMR 8502, 91405 Orsay Cedex, France

ARTICLE INFO

Keywords:
Manganese oxide
Vernadite
Birnessite
Pair distribution function
Nickel
Transmission electron microscopy

ABSTRACT

In-situ kinetics and mechanisms of Ni^{2+} uptake by synthetic vernadite were determined at pH 5.8 and I = 0.1 M NaCl using wet chemistry, atomic-resolution scanning transmission electron microscopy coupled with electron energy loss spectroscopy (STEM-EELS) and synchrotron high-energy X-ray scattering (HEXS) in both the Bragg-rod and pair distribution function formalisms. The structural formula of the initial solids was $^{TC}Mn^{3+}_{0.05}Na^{+}_{0.23}(H_2O)_{0.69}H^{+}_{0.06}[(Mn^{4+}_{0.86}Mn^{3+}_{0.04}vac_{0.1})O_2]$, where species under brackets form the layer having "vac" layer vacancies, and where other species are present in the interlayer, with TC standing for "triple-corner sharing" configuration. According to HEXS and STEM-EELS, adsorbed Ni^{2+} adopted mainly a TC configuration, and had a Debye-Waller factor about four times higher than layer Mn. Steady-state was reached after ~2.2 h of contact time, and the final structural formula of the solid was $^{TC}Ni^{2+}_{0.12}{}^{TC}Mn^{3+}_{0.05}Na^{+}_{0.12}H_2O_{0.36}H^{+}_{0.01}[(Mn^{4+}_{0.87}vac_{0.13})O_2]$. Atomic-scale imaging of the solids also evinced the presence of minor Ni adsorbed at the crystal edge. The retention coefficient $R_D = 10^{3.76\ \pm\ 0.06}$ L kg^{-1}, computed from PDF data modelling and solution chemistry results, was in agreement with those available in the literature.

1. Introduction

Vernadite, a manganese (Mn) oxide, is ubiquitous in the environment, being found as nodules and coatings in soil and sediments or as rock varnishes in deserts and polar and temperate regions (Bargar et al., 2009; Burns and Burns, 1977; Chukhrov et al., 1985; Dorn, 1991; Dorn et al., 1992; Dorn and Oberlander, 1981; Exon et al., 2002; Fuller and Bargar, 2014; Glover, 1977; Manceau et al., 2003, 2004; Marcus et al., 2004; Palumbo et al., 2001; Potter and Rossman, 1979). In surficial environments, vernadite precipitation by oxidation of aqueous Mn^{2+} in the presence of bacteria, fungi, and higher living forms (Grangeon et al., 2010; Lanson et al., 2008; Tani et al., 2003; Villalobos et al., 2003; Webb et al., 2005) is faster than abiotic oxidation catalysed by mineral surfaces by orders of magnitude (e.g. Hastings and Emerson, 1986; Tebo et al., 2004). Vernadite structure consists in the turbostratic stacking of layers made of $(Mn^{4+}O_6)^{8-}$ octahedra connected through their edges and separated from each other by hydrated interlayer cations (Giovanoli, 1980). These layers contain isomorphic substitutions of Mn^{4+} by cations of lower valences (e.g., Mn^{3+}, Ni^{2+}, Co^{2+}) and/or layer vacancies (Grangeon et al., 2008; Lanson et al., 2008; Villalobos et al., 2006), which induce a layer charge deficit reported to reach values as high as 1.6 valence unit (v.u.) per layer octahedron (Lanson et al., 2008). The layer charge deficit created by substituted octahedron (1 or 2 v.u. for trivalent and divalent octahedral cations respectively) is mostly compensated for by adsorbed hydrated cations forming outer-sphere complexes (e.g. Na^{+}, Ca^{2+}), while the layer charge deficit created by vacant Mn site (4 v.u.) is most frequently compensated for by adsorbed cations forming inner-sphere complexes above layer vacancies, in a triple-corner sharing (TC) configuration (e.g., Cu^{2+}, Mn^{3+}, Pb^{2+}, Zn^{2+} - Grangeon et al., 2012; Lanson et al., 2000, 2002b; Manceau et al., 2014; Peña et al., 2015). In addition, vernadite is nanocrystalline (Bargar et al., 2009) and its small particles have thus a large edge specific surface area, which bears a significant density of amphoteric reactive sites (Simanova et al., 2015). For all of these reasons, vernadite has high reactivity towards many trace elements and the geochemical cycle of many metals, rare-earth

* Corresponding author.
E-mail address: s.grangeon@brgm.fr (S. Grangeon).

http://dx.doi.org/10.1016/j.chemgeo.2017.03.035
Received 19 December 2016; Received in revised form 29 March 2017; Accepted 31 March 2017
Available online 31 March 2017

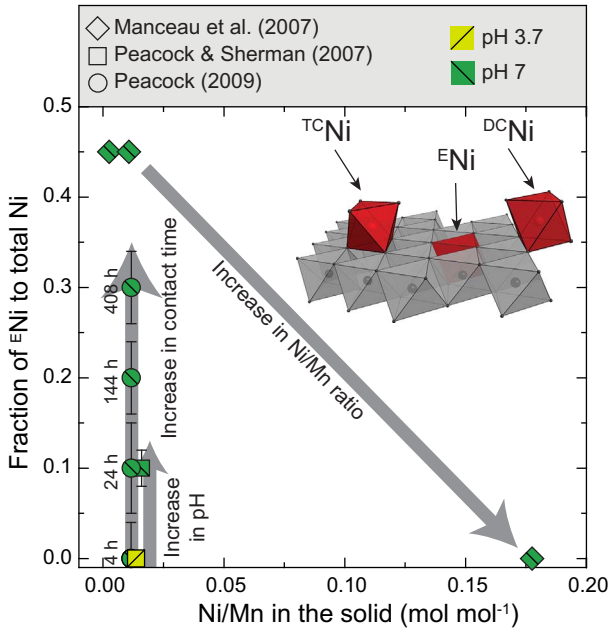

Fig. 1. Dependency of the abundance of ^{E}Ni to various environmental factors. Blue, yellow and green colours indicate that studies were conducted respectively at pH 3.7, 7 and 8. From left to right, arrows highlight the dependency of the abundance of ^{E}Ni on an increase in contact time, on Ni/Mn ratio, and on pH. The structure model drawn on the right schematizes the different configurations that Ni can adopt upon contact with vernadite. Red spheres and red octahedra materialize Ni and its coordination sphere respectively, while black spheres and grey octahedra materialize layer Mn and its coordination sphere respectively. (For interpretation of the references to colour in this figure legend, the reader is referred to the web version of this article.)

elements and actinides is controlled, or at least influenced, by vernadite in certain soils, freshwater and marine sediments (Koschinsky and Halbach, 1995; Manceau et al., 2000, 2004, 2007a; Marcus et al., 2004; Peacock and Moon, 2012; Peacock and Sherman, 2007a; Takahashi et al., 2007). Amongst metals, Ni^{2+} is of special interest, because of its toxicity (Kasprzak et al., 2003; Wang and Wang, 2008; Weng et al., 2004) and of its wide use in industrial processes and manures for agriculture (Nicholson et al., 2003).

Upon contact with vernadite, Ni^{2+} can adopt three main configurations (inset in Fig. 1): adsorbed at the particle edge in a double corner sharing configuration (^{DC}Ni), located above layer vacancies in a triple corner-sharing configuration (^{TC}Ni), or incorporated within the layer (^{E}Ni) (Grangeon et al., 2008; Manceau et al., 2007b; Peacock, 2009; Peacock and Sherman, 2007a,b; Peña et al., 2010). ^{E}Ni is favoured when surface coverage (i.e., Ni/Mn ratio) is low, when the pH of the equilibrium solution is alkaline, and when contact time between solution and vernadite is long (Fig. 1).

In many environmental compartments, the interaction between Ni^{2+} in solution and vernadite takes place in open chemical system where contact time is limited. These include streams, rivers, or the critical zone in soils. The kinetics of Ni^{2+}-vernadite interactions which certainly greatly influence the capacity of vernadite to uptake Ni^{2+} in these systems remain however largely undocumented. The importance of quantifying the kinetics of trace elements interaction with vernadite was discussed by Lopano and coworkers (Lopano et al., 2009, 2011) who studied the rates of exchange of Na^{+} by Ba^{2+}, Cs^{+} and K^{+} on synthetic birnessite, a three-dimensionally ordered phyllomanganate. Exchange processes were fast as samples reached equilibrium in the first hour of contact time, but only adsorption in the interlayer as outer-sphere complex could be probed because the authors used a birnessite with orthogonal layer symmetry, which contains very little layer vacancies, thus hindering the formation of inner-sphere complexes (Lanson et al., 2002a). The relevance of using such birnessite variety as a proxy for naturally-occurring vernadite may be questioned as this latter generally has hexagonal layer symmetry, as a result of a lower abundance of layer Mn^{3+} and of the frequent presence of layer vacancies (Bargar et al., 2009; Bodeï et al., 2007; Lanson et al., 2000; Manceau et al., 2014; Peacock and Sherman, 2007a; Wegorzewski et al., 2015).

This study aims at elucidating the mechanisms and quantifying the kinetics of Ni^{2+} uptake by vernadite. Synchrotron high-energy X-ray scattering followed by analysis in both Bragg-rod and pair distribution function formalisms made it possible to monitor sorption processes as a function of reaction time. These processes were further confirmed with atomic-resolution scanning transmission electron microscopy (STEM) coupled with energy electron-loss spectroscopy (EELS).

2. Materials and methods

2.1. Synthesis of the sample and chemical characterization

Synthetic vernadite (δ-MnO_2) was synthesized using the redox method (Villalobos et al., 2003). Briefly, a solution made of ~40 g $KMnO_4$ dissolved in ~1.3 L of deionized water was added to a solution made of 28 g NaOH dissolved in 1.4 L of deionized water. Then, a solution made of ~75 g $MnCl_2{\cdot}4H_2O$ was added, leading to the precipitation of synthetic vernadite which was separated from the solution by 10 series of centrifugation and Na saturation using a 1 M NaCl solution. The obtained Na-saturated synthetic vernadite was freeze-dried. An aliquot of the powder was used for the determination of the average Mn oxidation state (Mn AOS), using a potentiometric method (Grangeon et al., 2012).

2.2. High-energy X-ray scattering

High-energy X-ray scattering (HEXS) experiments were performed at station ID22 from the European Radiation Synchrotron Facility (ESRF, Grenoble, France), using energy of 69.9 keV and a Perkin Elmer XRD 1611CP3 flat detector. A polyimide capillary (diameter of 1.6 mm) was filled with synthetic vernadite, sealed on its two extremities using a frit-in-a-ferrule system (Idex Health & Science), and fixed in its measurement position. It was connected on one side to a peristaltic pump, used to flow the Ni^{2+} solution through the capillary, and to the other side to a waste container, using silicon tubing. A scheme of a similar set-up is available elsewhere (Marty et al., 2015). Flow rate was set to 20 mL h^{-1}. The input solution had a pH of 5.8 and contained 2 10^{-4} M $NiCl_2$ in a 0.1 M NaCl ionic background, so as to remain in chemical conditions comparable to previously published data (Tonkin et al., 2004). Recording of data started as soon as the solution was allowed to flow. An acquisition step consisted in the successive recording of 20 frames (5 s collection time each) and lasted 5 min, because of the need to record detector's dark current. Each acquisition step was separated from the next one by a dwell time of 2 min. The 20 frames acquired at each step were averaged and integrated using the pyFAI package (Ashiotis et al., 2015). The same procedure was applied to the recording of the signal arising from a capillary containing solely the aqueous solution. Data were transformed to X-ray pair distribution function (PDF) data using $PdfGetX_3$ (Juhas et al., 2013), with the contribution from the capillary and the aqueous solution being removed at this step. PDF data modelling was performed using PDFGui (Farrow et al., 2007). Turbostratism influences the PDF by attenuating the correlations resulting from pairs of atoms located on distinct layers as compared to those originating from atoms located on the same layer (Grangeon et al., 2015; Manceau et al., 2013). To circumvent this problem, the *r* interval of the simulation was restrained to the 1.2–7.2 Å range, i.e. to distances smaller than the layer-to-layer distance, using the model from Manceau and coworkers (Manceau et al., 2013). The atomic coordinates of ^{TC}Ni and its coordination sphere were constrained from the qualitative analysis of PDF data (see below). During the modelling of the first PDF (collected on the sample before it was